Anomalous Slowdown of Polymer Detachment Dynamics on Carbon Nanotubes

Daniel A. Vega,[1] Andrey Milchev,[2] Friederike Schmid,[2,1] and Mariano Febbo[1]

[1] *Instituto de Física del Sur (IFISUR) and Departamento de Física, Universidad Nacional del Sur (UNS), Consejo Nacional de Investigaciones Científicas y Técnicas - CONICET, Av. L. N. Alem 1253, 8000 - Bahía Blanca, Argentina**

[2] *Institute of Physics, Johannes Gutenberg University Mainz, Staudingerweg 7, 55128 Mainz, Germany†*

The "wrapping" of polymer chains on the surface of carbon nanotubes allows to obtain multifunctional hybrid materials with unique properties for a wide range of applications in biomedicine, electronics, nanocomposites, biosensors and solar cell technologies. Here we study by means of molecular dynamics simulations the force-assisted desorption kinetics of a polymer from the surface of a carbon nanotube. We found that due to the geometric coupling between the adsorbing surface and the conformation of the macromolecule, the process of desorption slow down dramatically upon increasing the windings around the nanotube. This behaviour can be rationalized in terms of an overdamped dynamics with a frictional force that increases exponentially with the number of windings of the macromolecule, resembling the Euler-Eytelwein mechanism that describe the interplay between applied tension and frictional forces on a rope wrapped around a curved surface. The results highlight the fundamental role played by the geometry to control the dynamics and mechanical stability of hybrid materials in order to tailor properties and maximize performance.

From ancient times up to nowadays, the interplay of the frictional forces and the tension on a rope wrapped around a solid support or another rope has been employed in a myriad of applications. Indeed, the first use of ropes for hunting, pulling, lifting, climbing, fastening, etc. is believed to date back to prehistoric times and predates the use of the axe (6000 BC) or the wheel (5000 BC) and probably, even the controlled use of fire (125000 BC) [1]. Winding a rope around a curved surface not only allows to transmit an applied force along a different direction, but also to strongly reduce the tension from one end to the other. This feature has been exploited in Leonardo da Vinci's machines or in tools dating back as far as ancient Egypt, and it is also employed in nature by tendril-producing plants [2, 3], like grape or passionflowers, and exploited by different mammals with prehensile tails, like the harvest mouse or New World monkeys, to hold on to branches (see Fig. 1), climb trees, and grab or manipulate objects [4].

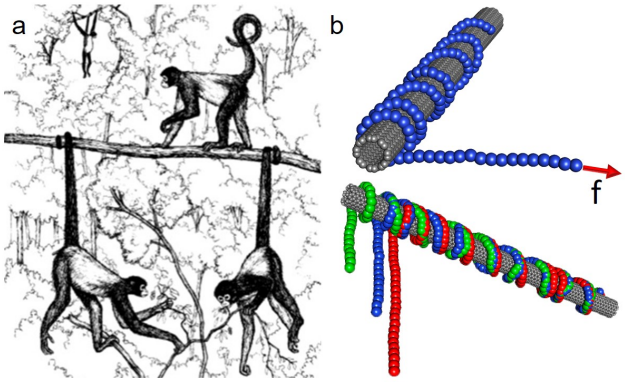

FIG. 1. Interplay between tension and friction on the macro and nanoscale. a)- Black spider monkeys (Ateles paniscus) can use their prehensile tails to hold onto branches. The friction between the prehensile tail and the surface of the branch is strongly enhanced due to its helical wrapping around the branch (adapted from Ref. [4]). b)- Macromolecule adsorbed on a nanotube partially detached by the presence of an external force **f** acting on one of the chain ends. Here we consider external forces that point along the direction perpendicular to the tube axis. The lower panel shows the polymer configuration at three different desorption times.

Geometrical properties are also relevant on the nanoscale, for example when considering the interactions between macromolecules and carbon nanotubes. "Wrapping" polymer chains around the surface of single wall carbon nanotubes (SWCNTs) allows to control their solubility in different solvents and also to create novel materials for materials science [5–10], medicine [11–13], biosensor technology [14], DNA sequencing [15, 16], and nanoelectronics [17]. For example, short sequences of single-stranded DNA can be employed to sort SWCNTs by diameter, chirality, or electronic behaviour, and hybrid nanomaterials combining biopolymers with SWCNTs have recently been utilized in a variety of applications such as drug delivery, imaging and sensing [18–20]. Using hybrid materials in applications requires a solid knowledge about the stability of the assembly depending on the conformation, the molecular size and the binding energy [18–21].

For example, the thermal stability of DNA-SWCNT hybrids was found to increase sharply with increasing DNA sequence length [22]. Depending on the architecture of the molecule, the self-organized structures and winding of the molecule around the tube can be controlled. For example, polysaccharide chains like chitosan [23] or phenylene-ethylene [24] polymers adopt a helical conformation when adhered to SWNTs while DNA makes a complete right-handed helical wrap around the SWCNT [18].

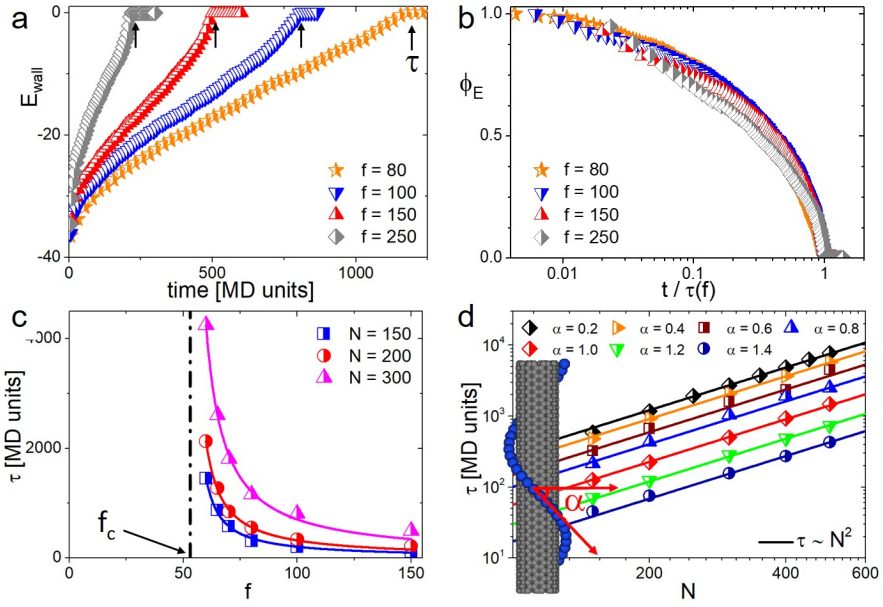

FIG. 2. Dynamics of force-assisted polymer desorption. a) Average polymer/nanotube energy of interaction per monomer E_{wall} as a function of time ($N = 300$, $\alpha = 1.0$). The time where $E_{wall} = 0$ determines the characteristic time for complete desorption, τ ($N = 300$, $\alpha = 1.0$). b)- Fraction of desorbed beads ϕ_E as a function of the rescaled time $t/\tau(f)$. c) Average desorption time τ vs. applied force f, plotted for different chain lengths N. Here the lines shows that τ diverges at a critical force $f_c \sim 52$ as $\tau \sim (f - f_c)^{-1}$ (helix pitch $\sim 31.5b$ and ~ 37 monomers/turn). d)- τ vs. chain size N for different helical conformations ($f = 150$). The lines show fits to $\tau \sim N^2$. Here α characterizes the pitch of the helical polymer conformation (see inset).

As a first step towards understanding the leading factors that control the mechanisms of desorption of a polymer chain from a carbon nanotube, here we use Molecular dynamics (MD) simulations of a coarse grained model to study the role of the geometry of the adsorbing surface on the dynamics of force-assisted polymer detachment (see Fig. 1b). Our central finding can be summarized as follows: We demonstrate the existence of a geometrically controlled friction phenomenon that drastically slows down the desorption process. We analyse this effect quantitatively and show that it is closely related to the capstan mechanism – a well-known macroscopic phenomenon that is relevant for many human activities. Hence we show that the same mechanism may also control the interactions of hybrid materials at the nanoscale, and thus unveil universal aspects of the phenomenon.

To investigate the mechanisms of force-assisted desorption, we consider polymers with different conformations that are absorbed on the surface of a SWCNT with a honeycomb structure in the armchair configuration. In order to investigate the geometric effect of the nanotube curvature, we choose a system with a relatively small tube diameter (0.55 nm considering the bond length of carbon atoms as 1.44) [17, 25]. The good solvent condition is implicitly implemented by using purely repulsive nonbonded interactions of the Weeks-Chandler-Anderson (WCA) type: $U^{WCA}(r) = 4\epsilon\left[\left(\frac{\sigma}{r}\right)^{12} - \left(\frac{\sigma}{r}\right)^{6} + \frac{1}{4}\right]$, $r \leq b$ and $U^{WCA}(r > b) = 0$. Here ϵ and σ are the units of energy and length, respectively. The parameter σ fixes bond length at equilibrium ($b = 2^{1/6}\sigma \approx 1.12$) and ϵ is expressed in units of k_BT, where k_B is the Boltzmann constant and T is the temperature [26]. The "MD units" of our paper are given in terms of σ and k_BT. In our MD simulations we use a coarse-grained model of a polymer chain of N beads connected by finitely extendable elastic bonds [27] (see Fig. 1b). The bonded interaction between the neighbour monomers along the polymer chain is described by the finitely extensible nonlinear elastic (FENE) potential, $U_{\rm FENE}(r) = -\frac{1}{2}kr_0^2 \ln\left[1 - \frac{r^2}{r_0^2}\right]$, $r \leq r_0$ and $U_{\rm FENE}(r > r_0) = \infty$, with $k = 30\,\varepsilon/\sigma^2$ and $r_0 = 1.5\,\sigma$. The chain stiffness is controlled by the bending potential: $U_{\rm bend}(\theta) = \kappa(1 - \cos\beta)$, where β is the bond angle formed between two subsequent bond vectors. The bending stiffness is controlled through the parameter κ. The attractive interaction of the chain beads with the tube is given by the conventional Lennard-Jones potential with a cutoff of 2.5σ in the MD code. Here we use the model parameters $\kappa = 15k_BT$ with $k_BT = 1$.

The time evolution of polymer desorption is calculated by solving a Langevin equation of motion for the position $\mathbf{r}_i$ of each bead along the chain: $m\ddot{\mathbf{r}}_i = \mathbf{F}_i - \eta\dot{\mathbf{r}}_i + \mathbf{R}_i + \mathbf{f}\delta_{i,N}$, where $m = 1$ is the mass of the bead, $\mathbf{F}_i$ is the force

acting on monomer i due to the presence of the nanotube and other polymer beads, $\mathbf{R}_i$ is a random force related to the friction coefficient η by the fluctuation- dissipation theorem and the last term represents the external (constant) stretching force acting along the radial direction of the nanotube on one of the end beads (see more details in the supplementary information).

The mechanism of chain desorption is analysed by monitoring the average number of beads detached from the nanotube. Due to the short ranged nature of the surface interaction, the average fraction of beads detached from the nanotube $\phi_E(t)$ can be accurately determined from the interaction energy per monomer $E_{wall}(t)$ between the polymer and the surface of the nanotube as $\phi_E(t) = E_{wall}(t)/E_{wall}(0)$. The time evolution of the process of polymer desorption for different strengths of the pulling force f is shown in Fig. 2a. During the desorption process, $\mid E_{wall} \mid$ decays with time, while the average desorption time for complete detachment τ increases with decreasing f. Figure 2b shows the dependence of the average fraction of beads adsorbed on the nanotube ϕ_E as a function of the reduced time $t/\tau(f)$, where $\tau(f)$ is the total desorption time for a given strength of the pulling force f. Within this representation, the data corresponding to different desorption conditions roughly collapses on a single curve.

Depending on the applied force, at long times the chain is either completely adsorbed or completely detached from the surface of the nanotube. Figure 2c shows the desorption time τ as a function of the pulling force f for chains of different length. The polymer detaches if the force exceeds a critical value f_c, which is determined by the attractive surface potential and independent of the chain length and conformation. For given $f > f_c$, the desorption time τ increases with the size of the polymer chain; in addition, τ diverges as f approaches f_c according to a power law, $\tau \sim (f - f_c)^{-1}$. Figure 2d shows the behaviour of τ as a function the chain length N for helical conformations with different pitch angle α (see the scheme in the inset of Fig. 2d). For given α, τ follows a power law behaviour $\tau \sim N^2$.

In addition, τ also depends dramatically on the helical pitch α. The detachment times for chains of the same length can differ by more than one order of magnitude depending on the pitch angle.

This effect is further analysed in Fig. 3. In the following, we express the initial number of beads per turn in a chain as $n_0 \sim 2\pi R/b\cos(\alpha)$, where $R \sim 2.86 \pm 0.02$ is the average distance between the polymer beads and the center of the nanotube, and b the bond length. Thus, the initial number of windings is given by $n_w = N/n_0$. Figure 3a compares the time evolution of the fraction of desorbed monomers $\phi(t)$ for two systems with different number of windings n_w, but with the same chain size and pulling force. For the chain with the smaller number of windings around the tube ($n_w = 2.5$), complete desorption is reached after about 1400 MD time units. The desorption process slows down drastically for the system with $n_w = 14$, where only $\sim 20\%$ of the monomers are fully desorbed from the tube at the same time (i.e., 1400 MD time units). Fig. 3b shows that for a given N, τN^{-2} grows nearly exponentially with the number of windings.

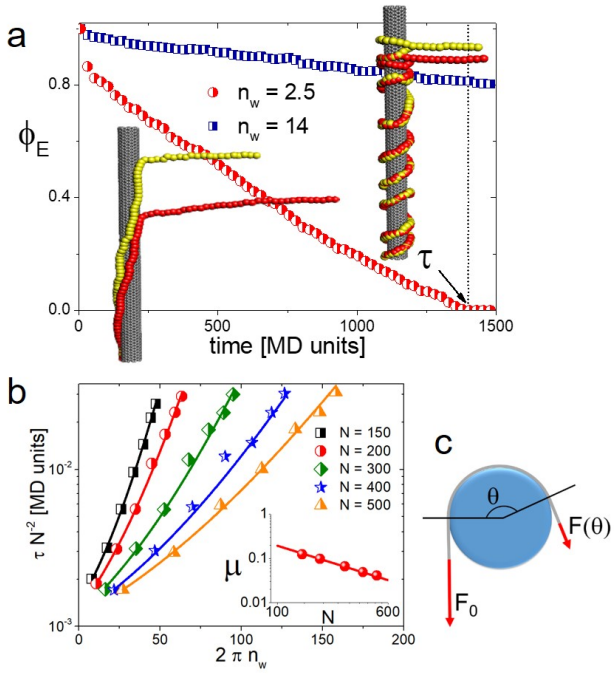

FIG. 3. Influence of the polymer conformation on the kinetics of polymer desorption. a)- Fraction of desorbed beads ϕ_E as a function of time. The insets show snapshots of the process of chain detachment at two times ($t = 25$ MD time steps: yellow beads and $t = 50$ MD time steps: red beads) for the two different polymer configurations. Note that the fraction of desorbed beads ϕ_E is strongly affected by the winding number n_w. Here $N = 300$ and $f = 60$. b) When plotted against the wrapping angle between the polymer and the nanotube $2\pi n_w$, it is found that τN^{-2} grows as predicted by eqn. 1 ($f = 150$). The inset shows that the effective friction with the tube surface decreases with N as $\mu \sim 1/N$. c)- According to the capstan model, for a inextensible rope at equilibrium, $F(\theta) = \exp(\mu\theta)F_0$.

The exponential dependence suggests that there might be a relation with the macroscopic phenomenon of belt friction, which occurs in situations where a rope is wrapped around a solid body. In that case, the equilibrium and dynamic properties depend on the rope configuration, the applied tension and the angle θ between the rope and the cylinder along the surface of contact. In the simplest case of an inextensible rope wrapped around a cylindrical drum, the problem is described by the Euler - Eytelwein formula [28–30] (also known as capstan equation): The applied tension F_0 decays exponentially with

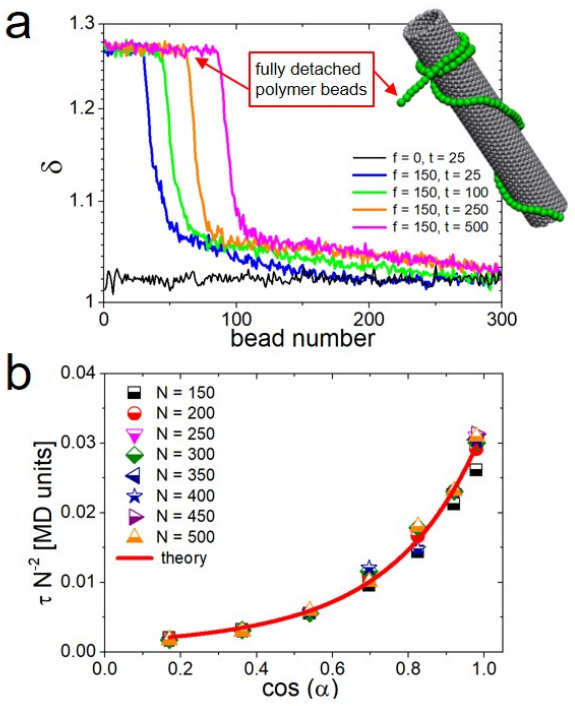

FIG. 4. Capstan-like dynamics of polymer desorption. a)-Average bond length deformation $\delta - \delta_0$ along the polymer chain at different simulation times ($\alpha = 0.6$). As a reference, this panel also shows the behaviour of δ in the absence of a pulling force. b) τN^{-2} vs. $cos(\alpha)$ (symbols) and theoretical prediction (line) for the data shown in Fig. 3b.

the friction coefficient between the rope and the surface μ and the total wrapping angle θ as $F(\theta) = F_0 \exp(-\mu\theta)$ (see the scheme in Fig. 3c). From rock climbing to belt machine design, this simple model has been widely used for more than 250 years. Figure 4a shows the behaviour of the bond length stretching $\delta - \delta_0$ along the contour length of the polymer chain during the process of desorption. Here δ_0 is the average bond length for a chain lying on the tube in the absence of a pulling force. While in the fully desorbed portion of the polymer chain the bond stretching is nearly constant, in the absorbed region $\delta - \delta_0$ decays rapidly along the polymer chain, in rough agreement with the capstan problem.

However, in contrast to macroscopic ropes, molecules in solution experience a substantial Stokes drag. To proceed, we will thus generalize the capstan equation to cases where the Stokes friction cannot be neglected. The tension at the nth chain bead is denoted $\gamma(n)$ (here $n = N$ corresponds to the free end and $n = 0$ to the end where the force f is applied). It is constant ($\gamma = (f - f_c)$) for the desorbed chain part and depends on n for $n < N - m(t)$, where $m(t)$ is the number of adsorbed beads at time t. The force acting on one bead in tangential direction due to the tension is thus $F_\gamma = \partial\gamma/\partial n$. In addition, in chain confined on a curved substrate, the tension generates a normal force $F_N = \gamma\frac{2\pi}{n_0}$ in the direction of the substrate. Due to this force, the bead experiences a solid friction force, which we approximate by Amonton's law, $F_\mu = \mu F_N$ with the kinetic friction coefficient μ. Finally, the Stokes friction force on the bead is given by $F_\zeta = \zeta v$ where ζ is the Stokes friction coefficient for a monomer moving on the surface of the tube, and $v = b|\frac{dm}{dt}|$ the average velocity of the chain. We consider an overdamped case where the velocity of the molecule results from a balance of forces, hence we require $F_\gamma + F_\mu + F_\zeta = 0$ for all beads with the boundary condition $\gamma(N) = 0$ at the free end of the molecule, and $\gamma(N - m(t)) = (f - f_c)$ at the detachment point. Combining everything (see supplementary information), the total desorption time can be expressed as

$$\tau_\mu = \tau_0\, g(2\pi\mu n_w) \text{ with } \tau_0 = \frac{\zeta b}{2}\frac{N^2}{f - f_c}, \qquad (1)$$

where $g(x) = \frac{2}{x^2}(e^x - x - 1)$. Note that in the limit $\mu \to 0$, the scaling of the desorption time, $\tau_\mu \to \tau_0 \propto N^2/(f - f_c)$, agrees with the scaling observed for the desorption process from a flat substrate [31]. Figure 3b also shows the results of a fit of the numerical data with the model equation Eqn. 1. In spite of its simplicity, the model captures the behaviour of τ vs. n_w and also the scaling observed in Figs. 2c and 2d.

The inset of 3b shows that the fitted values for the kinetic friction coefficient μ depend on the chain length and seem to decay as $\mu \sim \frac{\mu_0}{N}$. Taking this result into account in a heuristic manner and using $n_w = Nb\cos(\alpha)/2\pi R$, we obtain $\tau N^{-2} \propto g(\mu_0 b\cos(\alpha)/R)$. Fig. 4b shows that when τN^{-2} is plotted against $\cos(\alpha)$, all the data collapse onto a single curve with a functional form that is in excellent agreement with our model.

In summary, we have shown that the conformation of molecules adsorbed onto the surface of a carbon nanotube plays a crucial role for the dynamics of polymer detachment. In particular, wrapping molecules around the tubes can slow down the desorption dynamics by more than an order of magnitude. This effect might be important, e.g., for the kinetic stabilization of hybrid polymer-nanotube composites, where the interaction between different nanotubes is mediated by adsorbed polymers. The kinetic slowdown could also be exploited in applications such as DNA sequencing and SWCNT sorting.

ACKNOWLEDGEMENTS

The authors thank the Deutsche Forschungsgemeinschaft (Grants No. Schm 985/19 and No. SFB TRR 146),COST Action No. CA17139, supported by COST (European Cooperation in Science and Technology [33]),the National Research Council of Argentina (CONICET),and Universidad Nacional del Sur (UNS) for the financial support.

* dvega@uns.edu.ar
† Institute for Physical Chemistry, Bulgarian Academia of Sciences, 1113 Sofia, Bulgaria

[1] J. C. Turner and P. van de Griend, *History and Science of Knots* (World Scientific, 1996) https://www.worldscientific.com/doi/pdf/10.1142/2940.
[2] S. J. Gerbode, J. R. Puzey, A. G. McCormick, and L. Mahadevan, Science **337**, 1087 (2012).
[3] A. R. Studart and R. M. Erb, Soft Matter **10**, 1284 (2014).
[4] J. Fleagle and J. G. Fleagle, *Primate Adaptation and Evolution*, 3rd ed. (Academic Press, 2013).
[5] H. Fu, S. Xu, and Y. Li, Scientific Reports **6**, 30310 (2016).
[6] M. Zheng, A. Jagota, M. S. Strano, A. P. Santos, P. Barone, S. G. Chou, B. A. Diner, M. S. Dresselhaus, R. S. Mclean, G. B. Onoa, G. G. Samsonidze, E. D. Semke, M. Usrey, and D. J. Walls, Science **302**, 1545 (2003), http://science.sciencemag.org/content/302/5650/1545.full.pdf.
[7] M. Zheng, A. Jagota, E. D. Semke, B. A. Diner, S. R. L. Mclean, R. E. Richardson, and N. G. Tassi, Nature Materials **2**, 338 (2003).
[8] A. Karatrantos and N. Clarke, Soft Matter **7**, 7334 (2011).
[9] A. Karatrantos, R. J. Composto, K. I. Winey, M. KrÃűger, and N. Clarke, Macromolecules **45**, 7274 (2012), https://doi.org/10.1021/ma3007637.
[10] G. Allegra, G. Raos, and M. Vacatello, Progress in Polymer Science **33**, 683 (2008).
[11] L. Meng, X. Zhang, Q. Lu, Z. Fei, and P. J. Dyson, Biomaterials **33**, 1689 (2012).
[12] H. Meng, K. Andresen, and J. V. Noort, **43**, 3578 (2015).
[13] S. Prakash, M. Malhotra, W. Shao, C. Tomaro-duchesneau, and S. Abbasi, Advanced Drug Delivery Reviews **63**, 1340 (2011).
[14] D. A. Heller, H. Jin, B. M. Martinez, D. Patel, B. M. Miller, T. K. Yeung, P. V. Jena, C. Höbartner, T. Ha, S. K. Silverman, and M. S. Strano, Nature Nanotechnology **4**, 114 (2009).
[15] N. Yang and X. Jiang, Carbon **115**, 293 (2017).
[16] X. Tu, S. Manohar, A. Jagota, and M. Zheng, Nature **460**, 250 (2009).
[17] H. Wang, G. I. Koleilat, P. Liu, G. Jiménez-Osés, Y. C. Lai, M. Vosgueritchian, Y. Fang, S. Park, K. N. Houk, and Z. Bao, ACS Nano **8**, 2609 (2014).
[18] D. Roxbury, A. Jagota, and J. Mittal, The Journal of Physical Chemistry B **117**, 132 (2013).
[19] D. Roxbury, J. Mittal, and A. Jagota, Nano Letters **12**, 1464 (2012).
[20] D. Roxbury, A. Jagota, and J. Mittal, Journal of the American Chemical Society **133**, 13545 (2011).
[21] I. M. Kulić, H. Mohrbach, V. Lobaskin, R. Thaokar, and H. Schiessel, Phys. Rev. E **72**, 041905 (2005).
[22] D. Roxbury, X. Tu, M. Zheng, and A. Jagota, Langmuir **27**, 8282 (2011).
[23] Y. Liu, C. Chipot, X. Shao, and W. Cai, Journal of Physical Chemistry C **115**, 1851 (2011).
[24] C. D. Von Bargen, C. M. MacDermaid, O.-S. Lee, P. Deria, M. J. Therien, and J. G. Saven, The Journal of Physical Chemistry B **117**, 129531 (2013).
[25] X. Zhao, Y. Liu, S. Inoue, T. Suzuki, R. O. Jones, and Y. Ando, Phys. Rev. Lett. **92**, 125502 (2004).
[26] A. Ghosh, D. I. Dimitrov, V. G. Rostiashvili, A. Milchev, and T. A. Vilgis, The Journal of Chemical Physics **132**, 204902 (2010).
[27] G. S. Grest and K. Kremer, Phys. Rev. A **33**, 3628 (1986).
[28] L. Euler, *Methodus inveniendi lineas curvas maximi minimive proprietate gaudentes, sive solutio problematis isoperimetrici latissimo sensu accepti, Additamentum I (De curvis elasticis)* (Lausannæ, Genevæ, apud Marcum-Michaelem Bousquet & socios, 1744) pp. 245–320.
[29] L. Euler, Mem. Acad. Sci. Berlin , 265 (1769).
[30] J. A. Eytelwein, *Handbuch der Statik fester KÂĺorper. Mit vorzÂĺuglicher RÂĺucksicht auf ihre Anwendung in der Architektur*, Vol. 2 (Realschule Berlin, Berlin, 1808) pp. 245–320.
[31] J. Paturej, A. Milchev, V. G. Rostiashvili, and T. A. Vilgis, Macromolecules **45**, 4371 (2012).

SUPPLEMENTARY INFORMATION ON: ANOMALOUS SLOWDOWN OF POLYMER DETACHMENT DYNAMICS ON CARBON NANOTUBES

This document provides supplementary information about the microscopic model employed to describe the dynamics of polymer desorption and also additional results and details about the numerical simulations.

MODEL PARAMETERS AND STATISTICAL ERRORS.

The MD model parameters are selected as: $k_BT = 1$, $\eta = 0.25$, and $\kappa = 15$. The Verlet algorithm is used to integrate equations of motion using an integration step of 0.0005 time units (time is measured in units of $\sqrt{m\sigma^2/\epsilon}$).

We consider a nanotube with impenetrable walls and periodic boundary conditions along the tube axes ($z-$ direction). Initial helical configurations with different conformations were equilibrated by running 10^6 MD timesteps in the absence of an external force. Then, a force f was applied to the last monomer in the direction perpendicular to the adsorbing surface of the nanotube (radial direction).

Due to the attractive interaction potential between the polymer and the tube, the monomers that remain attached to the surface during the desorption process have an average distance of $(0.86 \pm 0.03)\sigma$ from the tube surface. Due to the symmetry of the problem and assuming that the tube is aligned along the z-axis, the average number of windings of the polymer chain around the nanotube can be expressed as: $n_w(t) = \frac{1}{2\pi}\sum_{i=1}^{N-1}\delta\theta_i$, where $\delta\theta_i = \theta_{i+1} - \theta_i$. Here θ_i represents the azimuthal coordinate corresponding to the $i-$bead of the polymer chain ($i = 1..N$).

Supplementary Figure 1 shows the desorption time τ as a function of the strength of the polymer/surface interaction parameter ϵ. For given $\epsilon > \epsilon_c$, the desorption time τ decreases with the strength of the pulling force; in addition, τ diverges as ϵ approaches a critical value ϵ_c according to a power law, $\tau \sim (\epsilon - \epsilon_c)^{-1}$. In this study we employed $\epsilon = 4$.

Supplementary Fig. 2 shows the average desorption time τ vs. the friction coefficient η in the Langevin dynamics simulations for $N = 200$ and $f = 150$. Note that within the model parameters explored in this study τ increases roughly linearly with η.

The results reported in Figs. 2 and 3 and 4b in the paper corresponds to the averages of 10 different configurations. The data corresponding to Fig. 4a was obtained by averaging 100 independent runs. As an example of the typical statistical errors associated to the average desorption time τ, the next table shows the values corresponding to systems containing $N = 200$ and $N = 400$ beads.

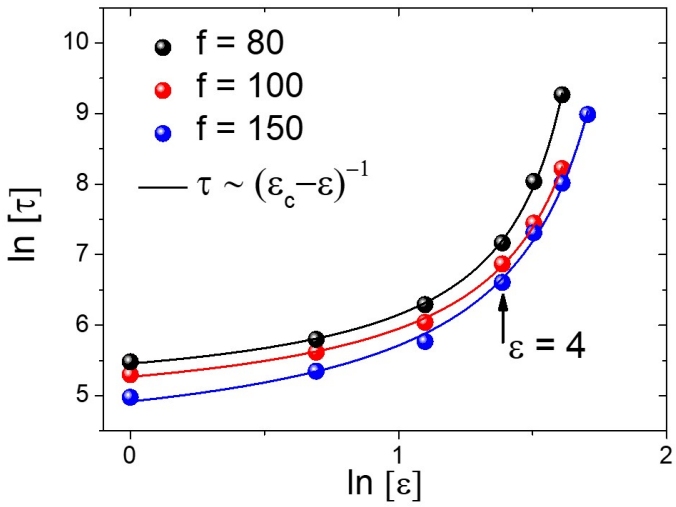

FIG. 1. Average desorption time τ vs. the strength of the attractive potential interaction parameter ϵ plotted for different applied forces. Here the lines shows that τ diverges as as $\tau \sim (\epsilon - \epsilon_c)^{-1}$ ($N = 250$; helix pitch $\sim 25.8b$).

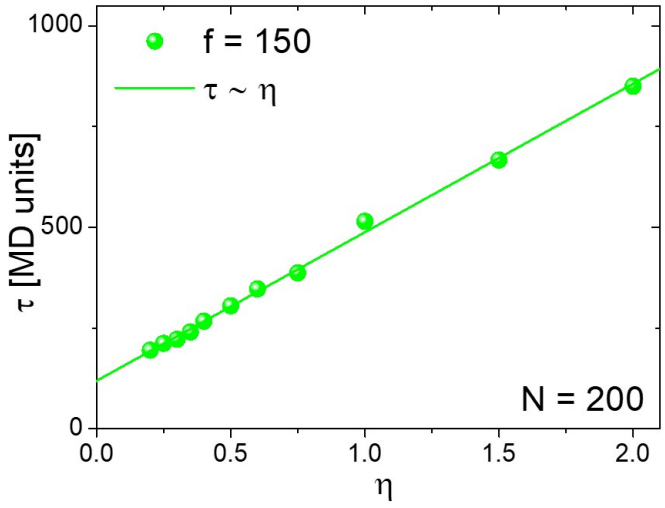

FIG. 2. Average desorption time τ vs. the friction coefficient η in the Langevin dynamics simulations. Here the continuous line corresponds to a linear interpolation through the numerical data

GENERALIZED CAPSTAN EQUATION

The force balance equation $F_\gamma + F_\mu + F_\zeta = 0$ results in the equation

$$\frac{\partial\gamma}{\partial n} + \mu\frac{2\pi}{n_0}\gamma = -\zeta v, \tag{2}$$

which is generally solved by

$$\gamma(n) = \zeta v\frac{1}{\mu_e}(e^{\mu_e(n^*-n)} - 1) \tag{3}$$

TABLE I. Average desorption time τ and its corresponding error $\Delta\tau$ for different values of α ($f = 150$).

α	$\tau(N=200)$	$\Delta\tau(N=200)$	$\tau(N=400)$	$\Delta\tau(N=400)$
0.2	0.0292	0.002	0.0305	0.001
0.4	0.0230	0.001	0.0231	7.9E-4
0.6	0.0167	0.001	0.0148	8.9E-5
0.8	0.0109	8.5E-4	0.0121	4.3E-4
1	0.0056	1.4E-4	0.0058	1.9E-4
1.2	0.0031	9.8E-5	0.0030	9.2E-5
1.4	0.0019	6.2E-5	0.0017	1.6E-5

with $\mu_e = \frac{2\pi\mu}{n_0}$ and an integration constant n^*. The latter is determined by the boundary condition $\gamma(N) = 0$ at the free end, giving $n^* = N$. The other boundary condition, $\gamma(N - m(t)) = (f - f_c)$, imposes a condition on the velocity v of the chain,

$$\zeta v = (f - f_c)\mu_e/(e^{\mu_e m} - 1). \tag{4}$$

Inserting $v = -b\frac{dm}{dt}$ and integrating, one obtains the implicit relation for $m(t)$

$$\frac{m(t)}{N}\sqrt{\frac{g(\mu_e m(t))}{g(\mu_e N)}} = \sqrt{1 - t/\tau_\mu} \tag{5}$$

with $g(x) = \frac{2}{x^2}(e^x - x - 1)$ and the total desorption time $\tau_\mu = \tau_0 g(\mu_e N)$ with $\tau_0 = \frac{N^2\zeta b}{2(f-f_c)}$ (corresponding to Eq. 1).

It is instructive to consider the limit $\mu \to 0$ and the limit $\zeta \to 0$. In the absence of solid friction, at $\mu \to 0$, one has $g(\mu_e N) \to 1$, thus the desorption time reduces to $\tau_\mu \to \tau_0$ and the number of adsorbed segments follows the simple relation

$$\frac{m(t)}{N} = \sqrt{1 - t/\tau_0}. \tag{6}$$

The limit $\zeta \to 0$ cannot be taken easily. Here, we have to reconsider the original equation (2), which then takes the form $\frac{\partial\gamma}{\partial n} + \mu\frac{2\pi}{n_0}\gamma = 0$. With the boundary condition $\gamma(N - m(t)) = (f - f_c)$, one obtains $\gamma(n,t) = (f - f_c)e^{-\mu_e(n-(N-m))}$. However, the boundary condition $\gamma(N,t) = 0$ cannot be met, hence the chain accelerates unless a force $F = (f - f_c)e^{-\mu_e m} = (f - f_c)e^{-\mu\theta}$ is applied at the free end, where $\theta = 2\pi m/n_0$ is the total wrapping angle. This corresponds to the original capstan equation.

DESORPTION DYNAMICS

Supplementary Fig. 3 shows the dynamics of polymer unwinding for a polymer chain with $N = 300$ beads. Here the average fraction of windings remaining on the nanotube at a given time t is given by: $\phi_w(t) = n_w(t)/n_w(t = 0)$. Similarly to the data shown in Fig. 2b in the paper, here we can also observe that data corresponding to different pulling forces roughly collapses in a single curve when plotted against t/τ.

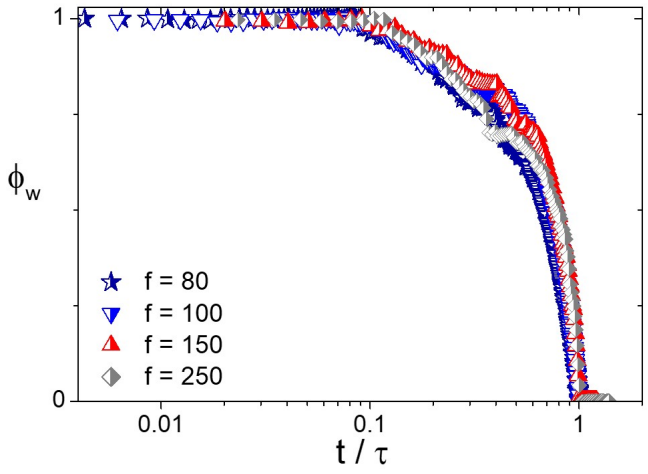

FIG. 3. Fraction of remaining windings ϕ_w during the force-assisted desorption process of a chain with $N = 300$ beads.

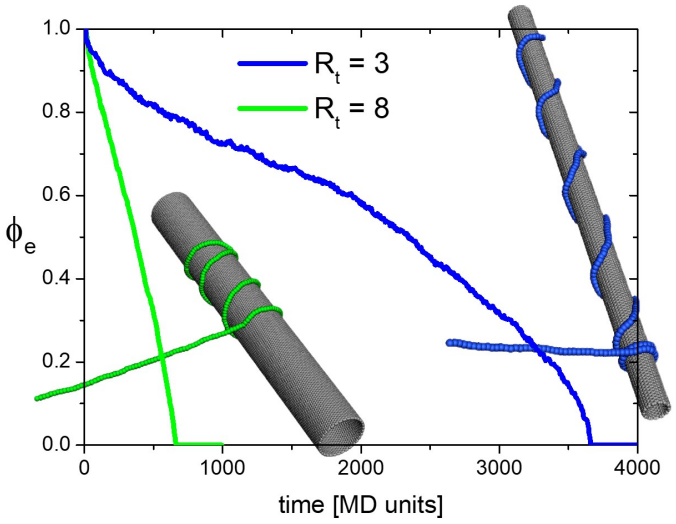

FIG. 4. Fraction of desorbed beads ϕ_E as a function of time for polymer chains adsorbed onto nanotubes with different diameters ($N = 300$). Note that the dynamics of polymer desorption is faster for a tube with a larger diameter ($R_t = 8\sigma$: green line; $R_t = 3\sigma$: blue line).

According to the Capstan model, for a given chain size N the number of windings decays as $1/R$, where R is the average distance between the polymer beads and the center of the nanotube. In our case, $R = R_t + \delta_s$, where R_t is the tube radius and $\delta_s \sim 0.86\sigma$ is the average distance between the adsorbed beads and the tube surface. Supplementary Figure 4 compares the dynamics of polymer desorption for a system evolving according to the

same set of model parameters as before but considering tubes with different diameters. Upon increasing R_t from $R_t = 3\sigma$ to $R_t = 8\sigma$, the desorption time τ reduces by a factor of $\tau^{Rt=8\sigma}/\tau^{Rt=3\sigma} \sim 0.18$ (see supplementary Fig. 4), in qualitative agreement with our model. However, it should be emphasized that the number of near neighbours accounting for polymer-surface interactions depends non-trivially on the tube diameter. Thus, the friction coefficient μ depends on tube diameter.